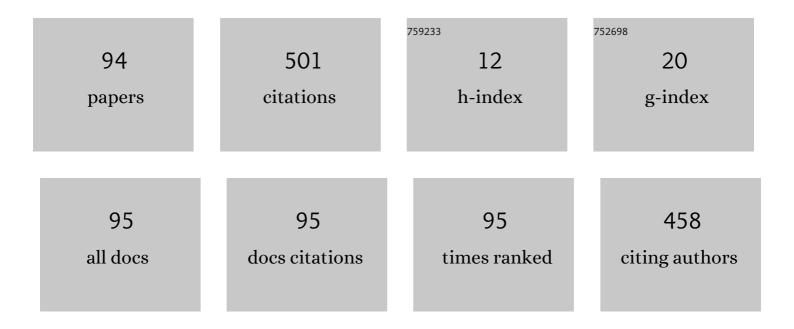
Holger Vogt

List of Publications by Year in descending order

Source: https://exaly.com/author-pdf/1440386/publications.pdf Version: 2024-02-01



HOLCEP VOCT

#	Article	lF	CITATIONS
1	A Novel Fully Implantable Wireless Sensor System for Monitoring Hypertension Patients. IEEE Transactions on Biomedical Engineering, 2012, 59, 3124-3130.	4.2	54
2	CMOS on buried nitride—A VLSI SOI technology. IEEE Transactions on Electron Devices, 1983, 30, 1515-1520.	3.0	51
3	Quality control of ultra-microelectrode arrays using cyclic voltammetry, electrochemical impedance spectroscopy and scanning electrochemical microscopy. Sensors and Actuators B: Chemical, 2001, 76, 573-581.	7.8	27
4	Characterization of buried silicon-nitride formed by nitrogen implantation. Nuclear Instruments & Methods in Physics Research B, 1987, 19-20, 279-284.	1.4	24
5	CMOS-compatible ruggedized high-temperature Lamb wave pressure sensor. Journal of Micromechanics and Microengineering, 2013, 23, 085018.	2.6	24
6	Integrated multi-sensor system for parallel in-situ monitoring of cell nutrients, metabolites, cell density and pH in biotechnological processes. Sensors and Actuators B: Chemical, 2016, 236, 937-946.	7.8	23
7	Lateral drift-field photodiode for low noise, high-speed, large photoactive-area CMOS imaging applications. Nuclear Instruments and Methods in Physics Research, Section A: Accelerators, Spectrometers, Detectors and Associated Equipment, 2010, 624, 470-475.	1.6	21
8	Ti/Ni(80%)Cr(20%) Thin-Film Resistor With a Nearly Zero Temperature Coefficient of Resistance for Integration in a Standard CMOS Process. IEEE Electron Device Letters, 2008, 29, 212-214.	3.9	18
9	On the design of a JFET-CMOS front-end for low noise data acquisition from microstrip detectors. Nuclear Instruments and Methods in Physics Research, Section A: Accelerators, Spectrometers, Detectors and Associated Equipment, 1988, 264, 391-398.	1.6	15
10	High Temperature Characterization up to 450°C of MOSFETs and Basic Circuits Realized in a Silicon-on-Insulator (SOI) CMOS Technology. Journal of Microelectronics and Electronic Packaging, 2013, 10, 67-72.	0.7	15
11	Integrated Multi-sensor System for Parallel In-situ Monitoring of Cell Nutrients, Metabolites and Cell Mass in Biotechnological Processes. Procedia Engineering, 2015, 120, 372-375.	1.2	14
12	Reliability of CMOS on Silicon-on-Insulator for Use at 250 \$^{circ}hbox{C}\$. IEEE Transactions on Device and Materials Reliability, 2014, 14, 21-29.	2.0	12
13	JFET-PMOS technology, in the design of monolithic preamplifier systems for multielectrode detectors. IEEE Transactions on Nuclear Science, 1991, 38, 69-76.	2.0	11
14	High quality silicon-on-insulator substrates by implanted oxygen ions. Materials Science and Engineering B: Solid-State Materials for Advanced Technology, 1989, 4, 429-433.	3.5	10
15	Enzyme Sensor With Polydimethylsiloxane Membrane and CMOS Potentiostat for Wide-Range Glucose Measurements. IEEE Sensors Journal, 2015, 15, 7096-7104.	4.7	10
16	With PECVD Deposited Poly-SiGe and Poly-Ge Forming Contacts Between MEMS and Electronics. Journal of Electronic Materials, 2019, 48, 7360-7365.	2.2	10
17	Reduction of heat loss of silicon membranes by the use of trenchetching techniques. Sensors and Actuators A: Physical, 1994, 42, 578-581.	4.1	9
18	The geometric design of microbolometer elements for uncooled focal plane arrays. , 2007, , .		9

#	Article	IF	CITATIONS
19	Performance of hydrogen-sensitive MOS capacitances with integrated on-chip signal conditioning. Sensors and Actuators B: Chemical, 1992, 6, 162-164.	7.8	8
20	Novel Approach to Defect Etching in Thin Film Siliconâ€onâ€Insulator. Journal of the Electrochemical Society, 1993, 140, 1713-1716.	2.9	7
21	Integration of vertical/quasivertical DMOS, CMOS and bipolar transistors in a 50 V SIMOX process. Microelectronic Engineering, 1992, 19, 733-735.	2.4	6
22	Encapsulation of implantable integrated MEMS pressure sensors using polyimide epoxy composite and atomic layer deposition. Journal of Sensors and Sensor Systems, 2014, 3, 335-347.	0.9	6
23	A miniature single-chip pressure and temperature sensor. Journal of Micromechanics and Microengineering, 1992, 2, 199-201.	2.6	5
24	A digital 25 Ã,µm pixel-pitch uncooled amorphous silicon TEC-less VGA IRFPA with massive parallel Sigma-Delta-ADC readout. , 2010, , .		5
25	Simulating Far-Infrared Scenarios with the Radiance Synthetic Imaging System. Computing in Science and Engineering, 2011, 13, 98-103.	1.2	5
26	Uncooled digital IRFPA-family with 17μm pixel-pitch based on amorphous silicon with massively parallel Sigma-Delta-ADC readout. , 2014, , .		5
27	Reliability of Microbolometer Thermal Imager Sensors Using Chip-scale Packaging. Procedia Engineering, 2015, 120, 1191-1196.	1.2	5
28	A technology concept for integrated detector electronics with CMOS compatible devices. Nuclear Instruments and Methods in Physics Research, Section A: Accelerators, Spectrometers, Detectors and Associated Equipment, 1987, 253, 434-438.	1.6	4
29	Measurement of SOI film thickness. Microelectronic Engineering, 1991, 15, 207-210.	2.4	4
30	Structural characterization of local SIMOX-substrates. , 1998, , .		4
31	PECVD of poly-SiGe/Ge layers with increased total gas flow. Microelectronic Engineering, 2014, 115, 26-31.	2.4	4
32	Study of enzyme sensors with wide, adjustable measurement ranges for in-situ monitoring of biotechnological processes. Sensors and Actuators B: Chemical, 2017, 241, 48-54.	7.8	4
33	Multi object detection in direct Time-of-Flight measurements with SPADs. , 2018, , .		4
34	Trends in VLSI technologies. Microelectronic Engineering, 1990, 12, 1-11.	2.4	3
35	Fabrication method for chip-scale-vacuum-packages based on a chip-to-wafer-process. , 2010, , .		3
36	Improvements of a digital 25 μm pixel-pitch uncooled amorphous silicon TEC-less VGA IRFPA with		3

Improvements of a digital 25 I¹/4m pixel-pitch uncooled massively parallel Sigma-Delta-ADC readout. , 2011, , .

#	Article	IF	CITATIONS
37	CMOS based capacitive biosensor with integrated tethered bilayer lipid membrane for real-time measurements. Biomedizinische Technik, 2012, 57, .	0.8	3
38	Thin-film SOI PIN-diode leakage current dependence on back-gate-potential and HCI traps. , 2015, , .		3
39	Modeling of the charge transfer in a lateral drift field photo detector. Solid-State Electronics, 2016, 126, 51-58.	1.4	3
40	Statistical tests to determine spatial correlations in the response behavior of PUF. , 2016, , .		3
41	Analytical model for thin-film SOI PIN-diode leakage current. Solid-State Electronics, 2017, 130, 4-8.	1.4	3
42	CMOS SiPM with integrated amplifier. Proceedings of SPIE, 2017, , .	0.8	3
43	Measurement concept for direct time-of-flight sensors at high ambient light. , 2019, , .		3
44	An improved electrical and thermal model of a microbolometer for electronic circuit simulation. Advances in Radio Science, 0, 10, 183-186.	0.7	3
45	Minimum oxygen dose for reliable application of SIMOX. Materials Science and Engineering B: Solid-State Materials for Advanced Technology, 1992, 12, 149-151.	3.5	2
46	<title>Modeling of microsystem flow sensor based on thermal time-of-flight mode</title> . , 2002, , .		2
47	CMOS process enhancement for high precision narrow linewidth applications. , 2010, , .		2
48	An uncooled VGA-IRFPA with novel readout architecture. Advances in Radio Science, 0, 9, 107-110.	0.7	2
49	Simulation method for LWIR radiation distribution using a visual ray-tracer. Optical and Quantum Electronics, 2012, 44, 297-301.	3.3	2
50	Failure mechanisms of microbolometer thermal imager sensors using chip-scale packaging. Microelectronics Reliability, 2015, 55, 1901-1905.	1.7	2
51	Measurement results of a 12 \hat{l} /4m pixel size microbolometer array based on a novel thermally isolating structure using a 17 \hat{l} /4m ROIC. , 2016, , .		2
52	Modeling of Thermal Conductivity for a CMOS-Compatible MEMS-ROIC Contact by TiN Nanotubes. IEEE Transactions on Electron Devices, 2019, 66, 3485-3491.	3.0	2
53	Modeling and Characterization of Adapted 3\$omega\$-Method for Thermal Conduction Measurement of Thermal Radiation Sensors. , 2020, 4, 1-4.		2
54	Digital uncooled IRFPAs based on microbolometers with 17 µm and 12 µm pixel pitch. , 2018, , .		2

#	Article	IF	CITATIONS
55	High-Temperature Trench Capacitors, Using Thin-Film ALD Dielectrics. Additional Conferences (Device) Tj ETQq1	1 0.784314 0.2	rgBT /Over
56	VB-7 performance of buried nitride CMOS devices. IEEE Transactions on Electron Devices, 1983, 30, 1606-1607.	3.0	1
57	SPICE modeling of resistive, diode, and pyroelectric bolometer cells. , 2006, , .		1
58	A new DC-temperature model for a diode bolometer based on SOI-pin-diode test structures. , 2010, , .		1
59	CMOS photodiodes for narrow linewidth applications. , 2011, , .		1
60	Sacrificial ion beam etching process for seed layer removal of 6 $^{1}\!4$ m pitch CuSn micro bumps. IOP Conference Series: Materials Science and Engineering, 2012, 41, 012005.	0.6	1
61	Microelectromechanical Implants: Encapsulation Concepts and Test Procedures. Biomedizinische Technik, 2012, 57, .	0.8	1
62	Reliability Investigations up to 350°C of Gate Oxide Capacitors Realized in a Silicon-on-Insulator CMOS Technology. Journal of Microelectronics and Electronic Packaging, 2013, 10, 150-154.	0.7	1
63	ALD-based 3D-capacitors for harsh environments. , 2016, , .		1
64	Optimization of the dielectric layer for electrowetting on dielectric. The Integration VLSI Journal, 2019, 67, 50-59.	2.1	1
65	D7.4 - CMOS integrated miniaturized photovoltaic cells for autonomous sensor nodes: simulations and experimental results. , 2015, , .		1
66	HOT-300 – A Multidisciplinary Technology Approach Targeting Microelectronic Systems at 300 °C Operating Temperature. Additional Conferences (Device Packaging HiTEC HiTEN & CICMT), 2016, 2016, 000001-000010.	0.2	1
67	High-performance uncooled digital 17 \hat{l} $\!/\!4$ m QVGA-IRFPA-using microbolometer based on amorphous silicon with massively parallel Sigma-Delta-ADC readout. , 2018, , .		1
68	Measurement concept to reduce environmental impact in direct time-of-flight LiDAR sensors. , 2020, , .		1
69	High-quality SOI-substrates for CMOS transistors. Vacuum, 1991, 42, 387-388.	3.5	0
70	Optimization of vertical 600 and 1500 V SOI-ESTs with low on-state voltages. Solid-State Electronics, 2000, 44, 2131-2138.	1.4	0
71	Synchronous discrete event simulation for fast and efficient simulation of a complete semiconductor factory. , 0, , .		0
72	A fast WLR Test for the evaluation of EEPROM Endurance. , 2009, , .		0

A fast WLR Test for the evaluation of EEPROM Endurance. , 2009, , . 72

#	Article	IF	CITATIONS
73	Light switched Plasma Charging Damage protection device allowing high field characterization. , 2009, , .		0
74	Noise of short-time integrators for readout of uncooled infrared bolometer arrays. Advances in Radio Science, 0, 8, 129-133.	0.7	0
75	Investigation of the temperature coefficient of electrical resistance and 1/f noise of laser-annealed amorphous silicon layers. , 2010, , .		0
76	Simulation method for LWIR radiation distribution using a visual ray-tracer. , 2011, , .		0
77	Light Switched Plasma Charging Protection Device for High-Field Characterization and Flash Memory Protection. IEEE Transactions on Device and Materials Reliability, 2011, 11, 81-85.	2.0	Ο
78	Posterausstellung P81-100. Biomedizinische Technik, 2011, 56, 1-22.	0.8	0
79	Quantum Efficiency Determination of a Novel CMOS Design for Fast Imaging Applications in the Extreme Ultraviolet. IEEE Transactions on Electron Devices, 2012, 59, 846-849.	3.0	Ο
80	Speed considerations for LDPD based time-of-flight CMOS 3D image sensors. , 2013, , .		0
81	Performance analysis of a large photoactive area CMOS line sensor for fast, time-resolved spectroscopy applications. Proceedings of SPIE, 2014, , .	0.8	Ο
82	Track B. Biomedizinische Technik, 2014, 59, s113-43.	0.8	0
83	Investigation of diaphragm deflection of an absolute MEMS capacitive polysilicon pressure sensor. , 2015, , .		Ο
84	Modeling of CMOS image sensors for time-of-flight applications. Proceedings of SPIE, 2015, , .	0.8	0
85	Materials and technologies to enable high temperature stable MEMS and electronics for smart systems used in harsh environments. , 2016, , .		Ο
86	Ungekühlte Mikrobolometer-Arrays mit einer Pixelgröße von 12â€Âµm basierend auf einer neuartigen thermisch isolierenden Struktur. TM Technisches Messen, 2017, 84, 381-388.	0.7	0
87	Fabrication and electrochemical characterization of ruthenium nanoelectrodes. Current Directions in Biomedical Engineering, 2017, 3, 393-396.	0.4	Ο
88	Simulation Results of Prospective Next Generation 3-D Thermopile Sensor and Array Circuitry Options. , 2018, 2, 1-4.		0
89	Monolithic Integration and Analysis of Vertical, Partially Encapsulated Nanoelectrode Arrays. Journal of Microelectromechanical Systems, 2020, 29, 1180-1188.	2.5	0
90	A Far Infrared VGA Detector Based on Uncooled Microbolometers for Automotive Applications. , 2011, , 327-334.		0

#	Article	IF	CITATIONS
91	Experimental reliability studies and SPICE simulation for EEPROM at temperatures up to 450 °C. Additional Conferences (Device Packaging HiTEC HiTEN & CICMT), 2015, 2015, 000005-000009.	0.2	0
92	Experimental Reliability Studies and SPICE Simulation for EEPROM at Temperatures up to 450°C. Journal of Microelectronics and Electronic Packaging, 2016, 13, 33-37.	0.7	0
93	1.1.2 - Entwicklung eines piezoresistiven Drucksensors für Hochtemperaturanwendungen auf Basis eines SOI-Substrats. , 2016, , .		0
94	4.1.3 - Ungekühlte Mikrobolometer-Arrays mit einer Picelgröße von 12 μm basierend auf einer neuartigen thermischen isolierenden Struktur. , 2016, , .		0